Geophysical Journal International

Geophys. J. Int. (2021) **226,** 1599–1614
Advance Access publication 2021 May 04
GJI General Geophysical Methods

doi: 10.1093/gji/ggab179

Seismic reflectivity and transmissivity parametrization with the effect of normal *in situ* stress

Fubin Chen, Zhaoyun Zong and Man Jiang

School of Geosciences, China University of Petroleum (East China), 66 *Changjiang West Road, Qingdao* 266580*, China. E-mail: zhaoyunzong@yahoo.com*

Accepted 2021 April 30. Received 2021 January 19; in original form 2020 September 16

SUMMARY

In situ stress has a significant effect on the properties of underground formations, including seismic wave velocity, porosity and permeability, and further affects seismic reflectivity and transmissivity. Research works on the effect of *in situ* stress are helpful to construct more precise seismic reflection and transmission coefficient equations. However, previous studies on seismic reflectivity equations did not take the effect of normal *in situ* stress into consideration. The mechanism of stress on seismic reflectivity and transmissivity is still ambiguous. In this study, we propose new explicit equations to help analyse the changes of seismic reflectivity and transmissivity under the effect of normal *in situ* stress. First, we deduce the Christoffel equation on the basis of solid acoustoelastic theory. Then, we utilize appropriate boundary conditions to formulate analytical equations of the reflectivity at the interface between two stressed formations, which can provide some new insights into the role of *in situ* stress. The shear wave birefringence will vanish because we assume that the wave propagates in the *X*–*Z* plane. Different rock models with different lithology and saturation are used to analyse the variation of seismic reflectivity and transmissivity with normal stress and incident angle at the interface. The main effect of normal stress on reflection and transmission coefficients is to change amplitude and critical incident angle. When the upper and lower layers are sandstones, the critical incident angle decreases with the increase of normal *in situ* stress, which is consistent with previous studies. In addition, the reflectivity equation can be degenerated to the Zoeppritz equation when the normal *in situ* stress vanishes, which further validates that the equation proposed is correct. Seismic reflectivity equations that couple the effect of stress can lay a foundation for direct prediction of *in situ* stress.

Key words: High-pressure behaviour; Numerical solutions; Acoustic properties; Wave propagation.

INTRODUCTION

Seismic reflection and transmission coefficient equations are the basis for formation property prediction, which is significant for fluid identification and reservoir prediction (Robert & Lloyd 1983; Wang 2012; Zong *et al.* 2013; Yin *et al.* 2015). The AVO (amplitude variation with offset) technology based on the Zoeppritz equation and its approximations has been well developed over the decades and widely applied in seismic exploration (Aki & Richards 1980; Shuey 1985; Fatti 1994; Chen *et al.* 2020). The target of seismic reflection and transmission gradually transforms from elastic, isotropic and homogeneous media to inelastic, anisotropic and heterogeneous media. This transformation makes the derived reflection and transmission equations more suitable for real underground formations. Even so, there are still some factors that have been ignored in the derivation of these equations, for example the *in situ* stress. *In situ* stress exists extensively underground, which has great effect on seismic wave velocity, porosity and permeability of the stratum, and further affects the seismic wave reflectivity and transmissivity at the stratum interface (Simmons 1964; Zhang 2013; Wang & Wang 2015). However, most of the former reflection and transmission coefficient equations were derived without considering the effect of *in situ* stress (Song *et al.* 2020). And it is widely believed that the accuracy of reflection and transmission coefficient equations can be improved through taking the effect of *in situ* stress into consideration.

Hughes proposed the third-order elastic modulus to describe the relationship between seismic wave velocity of the rock and stress (Hughes & Kelly 1953), and then a number of researchers began to study the solid acoustoelas-Kirchhoff stress tensor can ticity, that is the velocity of seismic wave changes with the change of stress. In the following decades, researchers have established a complete system of solid acoustoelastic theory that describes the nonlinear relation between strain and stress (Tatsuo & Masakatsu 1969;

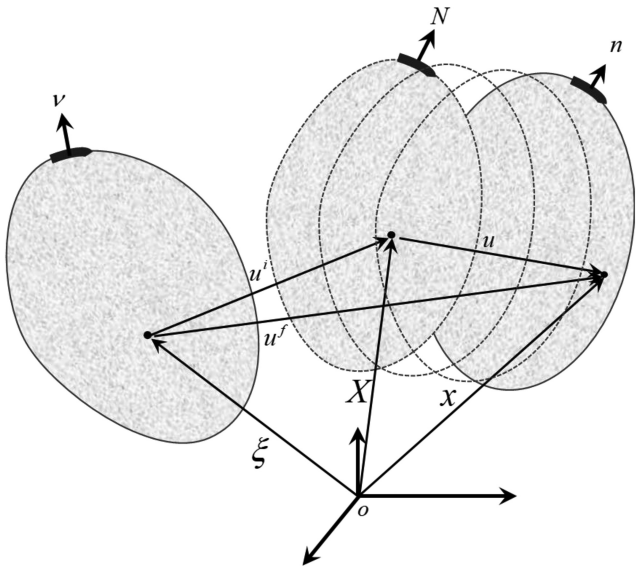

Figure 1. Coordinate systems for a pre-deformed rock point at the natural, initial and final configurations.

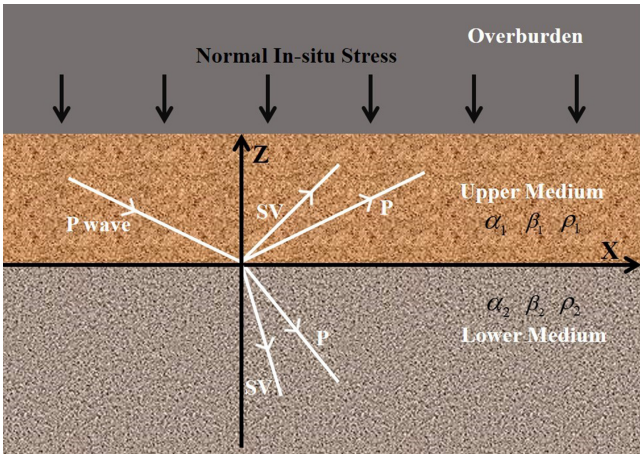

Figure 2. Reflection and transmission of seismic waves at the interface of two stressed strata.

Pao *et al.* 1984; Norris 1995; Abiza *et al.* 2012). Solid acoustoelasticity theory uses quantitative formulae to describe the relation between stress and seismic wave velocity in different directions, which lays a foundation for the derivation of seismic reflectivity and transmissivity equations considering the effect of *in situ* stress.

Birefringence occurs when seismic wave propagates to the interface separating two stressed solids, which means applied stress can make *S* wave split into fast S wave and slow S wave. Thus, the incident *P* wave would be converted to reflected *P* wave, reflected fast *S* wave, reflected slow *S* wave and transmitted *P* wave, transmitted fast *S* wave and transmitted slow *S* wave at the interface between two stressed solids (Pao *et al.* 1984; Degtyar & Rokhlin 1995). In this study, we assume that the transverse principal strains (e_{11} and e_{22}) are equal, so there will be no birefringence in the *X*–*Z* plane; that is the incident wave will only generate reflected *P* and *SV* waves, and transmitted *P* and *SV* waves at the interface between two stressed solids in the *X*–*Z* plane (Degtyar 1998).

Some physicists have studied the acoustic wave reflection and transmission at the interface between two stressed materials on the basis of solid acoustoelastic theory. The energy reflection coefficient equations at the interface between fluid and stressed aluminium, as well as between two stressed alloys, are established. And some other researchers have studied the amplitude reflection of stressed aluminium and alloy material (Degtyar 1998; Song 2020). With a similar derivation method, the energy reflection and transmission coefficient equations at the interface between fluid and a stressed rock were derived, followed by the establishment of the energy flow reflection and transmission coefficient equations at the interface between two rocks under transverse stress (Liu *et al.* 2010, 2012). However, the numerical expressions of amplitude reflection equations are not given. Moreover, the previous reflection equations at the interface with the effect of transverse stress were presented, failing to take vertical normal stress into consideration. It is necessary to establish the reflectivity equations under normal stress because underground rocks are subjected to normal stress caused by the gravity of the overlying formations in the field.

In the field of seismic exploration, researchers are greatly interested in the seismic amplitude reflection coefficient at the interface between two stressed strata, which gives us great motivation to establish seismic reflectivity and transmissivity equations considering the effect of *in situ* stress. These equations can be applied to make the prediction of *in situ* stress based on seismic data more accurate, more stable and faster than conventional empirical formulae from the logging and drilling data.

In this paper, we assume that seismic waves are plane waves and the strata are isotropic. We also assume that only normal *in situ* stress exists according to the actual stress distribution of the strata. Based on the theory of solid acoustoelasticity, we established the analytical reflectivity and transmissivity equations in the *X*–*Z* plane at the interface between two solids under normal stress, which can provide new insights into the effect of *in situ* stress. Then, we analyse the variation of seismic reflection and transmission coefficients with stress and incident angle at the interface between strata with different lithology and saturation. The results distinctly show that the normal stress has an important effect on the seismic reflection and transmission of the interface separating two strata with different lithology and saturation. The critical incident angle of *P* wave decreases continuously with the increase of *in situ* stress, which is consistent with the previous studies on acoustic energy reflection and transmission. In addition, the reflectivity and transmissivity equations can be degenerated to the traditional Zoeppritz equation when the *in situ* stress becomes zero, which further validates the accuracy of equations we proposed.

METHODOLOGY

Solid acoustoelastic theory

Rocks underground have undergone very complicated loading, unloading, heating and cooling processes that produce corresponding stresses and strains. The rock's state without stress and strain is called its natural state, and a rock in deformation or under stress is called its initial state. When a seismic wave motion is superposed on the rock in the initial state, the rock deforms to the final state. Physical variables of the natural, initial or final state are distinguished by the superscripts 0, i and f, respectively. And the positions of a

Table 1. Rock samples properties.

		Rock							
Property	Saturation state	Portland sandstone	Indiana limestone	Granite	Berea1 sandstone	Berea2 sandstone	Berea3 sandstone	Castlegate sandstone	Tight rock
Compressional velocity ($m\,s^{-1}$)	Dry	2190	3730	4599	2051	2644			4677.6
	Saturated	3234	4216		2841	3230	3022	2000	4899.0
Shear velocity ($m\,s^{-1}$)	Dry	1948	2216	2865	1423	1761			2988.5
	Saturated	1726	2166		1340	1855	1745	1275	3042.4
Density ($kg\,m^{-3}$)	Dry	2140	2210	2638	2040	2100			2600
	Saturated	2330	2390		2280	2310	2135	2000	2622
A (GPa)	Dry	−268	−10 550	125 030	−316	−1206			−6839
	Saturated	−3692	−18 754		−17 574	−27 470	−1541	−95.9	−4544
B (GPa)	Dry	−161	−5643	−54 303	−1692	−1437			0
	Saturated	−1310	−11 715		−4939	−13 723	193	−162.5	0
C (GPa)	Dry	−418	−985.7	15 318	−1252.8	−1409.3			−1564.5
	Saturated	−590.5	−1639.8		558.5	−2295.7	−385.5	−340.8	−872

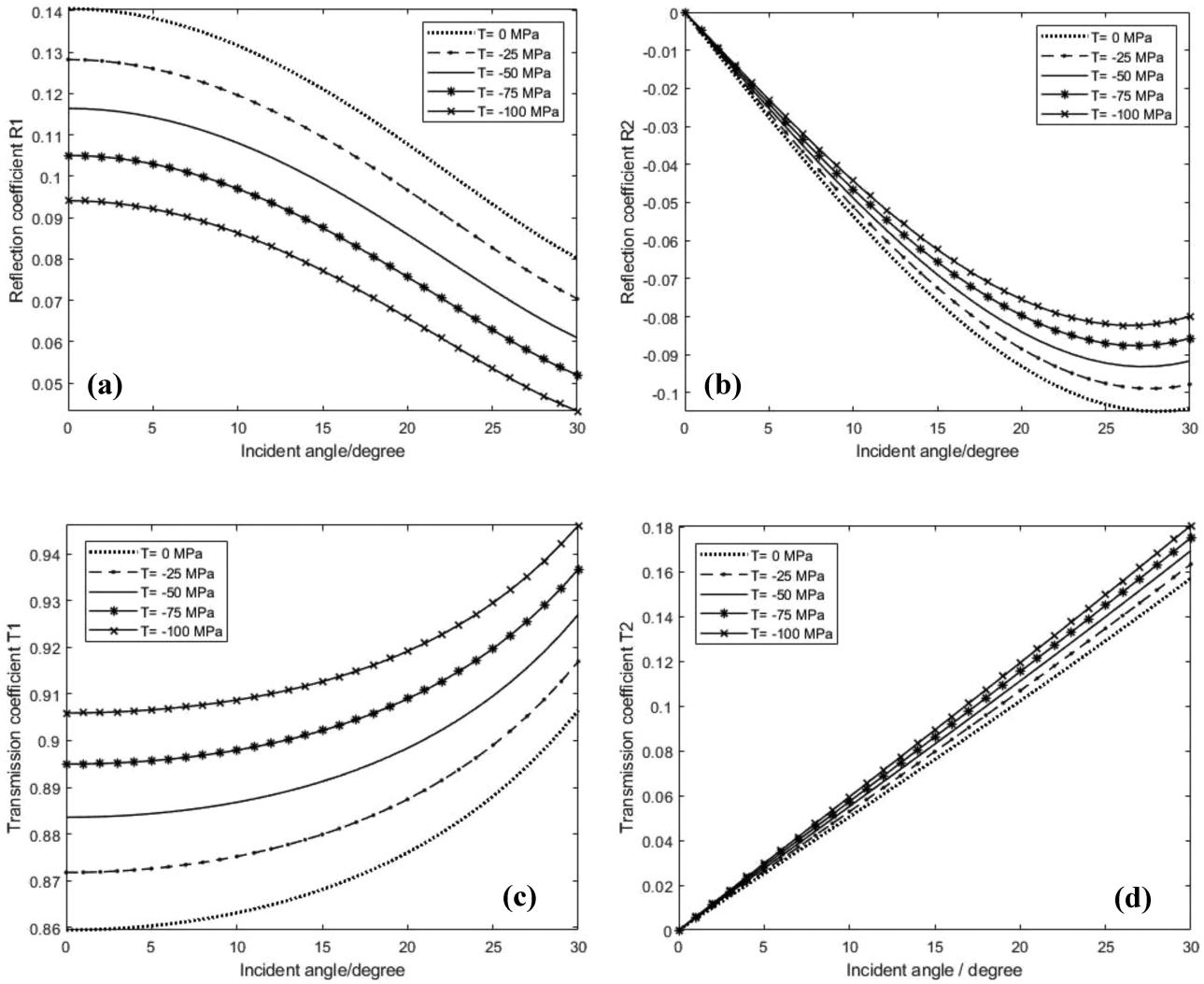

Figure 3. The seismic reflection coefficients and transmission coefficients at the interface between dry Berea1 sandstone and dry Berea2 sandstone under normal *in situ* stress. The dotted, dashed, solid, star marked and cross marked lines denote unstressed state, −25, −50, −75 and −100 MPa in rocks, respectively. (a) Reflection coefficient of *P* wave, (b) reflection coefficient of *SV* wave, (c) transmission coefficient of *P* wave and (d) transmission coefficient of *SV* wave.

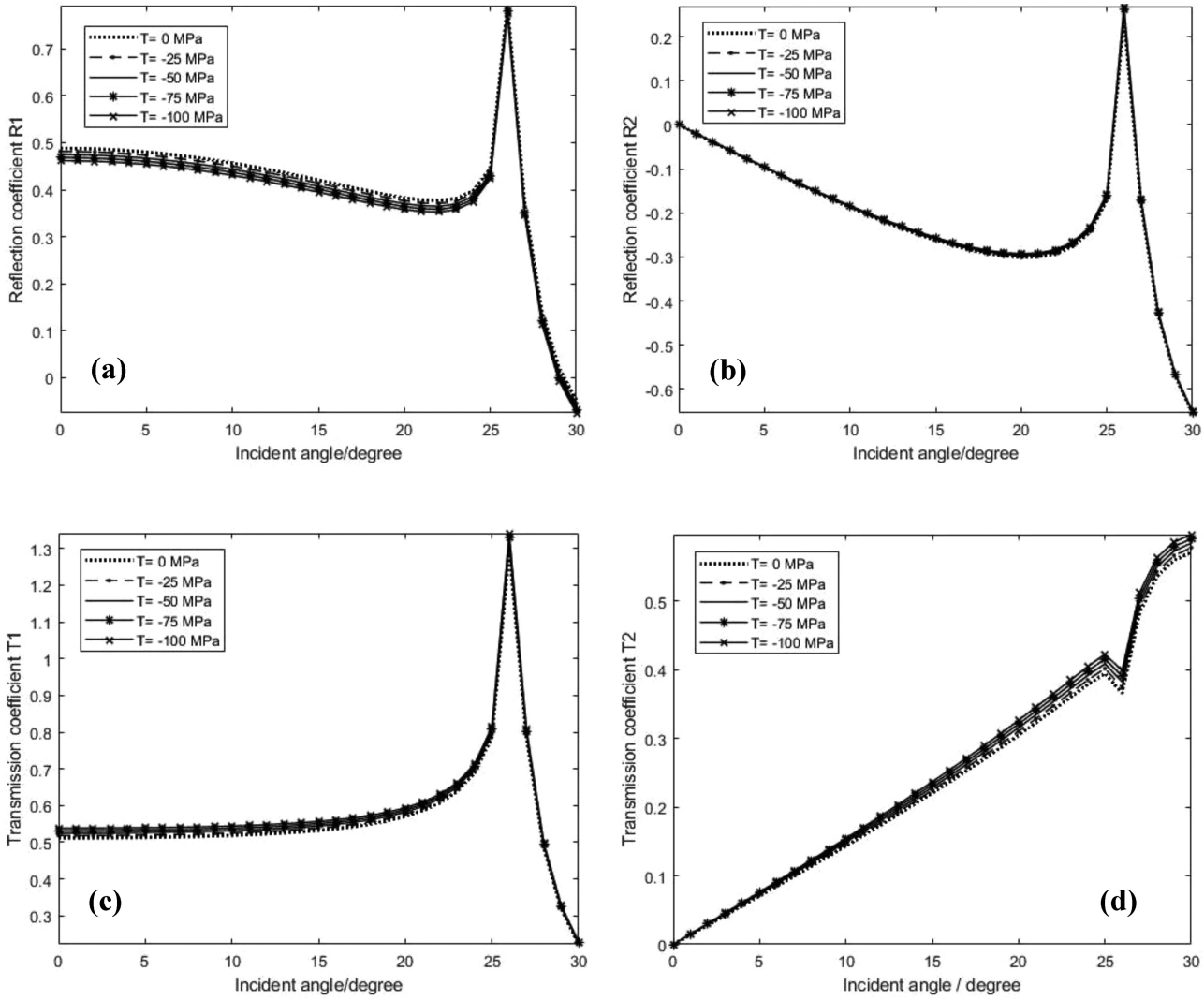

Figure 4. The seismic reflection coefficients and transmission coefficients at the interface between dry Berea1 sandstone and dry tight rock under normal *in situ* stress. The dotted, dashed, solid, star marked and cross marked lines denote unstressed state, −25, −50, −75 and −100 MPa in rocks, respectively. (a) Reflection coefficient of *P* wave, (b) reflection coefficient of *SV* wave, (c) transmission coefficient of *P* wave and (d) transmission coefficient of *SV* wave.

particle inside the rock at its natural, initial and final states are determined by position vectors ξ, X and x, respectively, which direct from the origin of a common Cartesian coordinate system (Tian & Wang 2006), as shown in Fig. 1.

By introducing the third-order elastic modulus, the solid acoustoelastic theory constructs a nonlinear stress–strain relationship and describes the motion process of a solid particle under the effect of stress. The static displacement of rock particles from the natural state to the initial state is u^{i}, and displacement from the natural state to the final state is u^{f}. The relations between displacements and position vectors are as follows:

$$u^{\mathrm{i}}(\xi) = X - \xi, \tag{1}$$

$$u^{\mathrm{f}}(\xi, t) = x - \xi. \tag{2}$$

The displacement increment from the initial state to the final state caused by seismic wave perturbation is the difference between eqs (1) and (2), as

$$u(\xi, t) = x - X = u^{\mathrm{f}} - u^{\mathrm{i}}. \tag{3}$$

The deformation of a rock particle in adjacent state can be measured by the deformation gradient. The Lagrangian strain of a rock particle at the initial state and final state in the natural coordinate system can be obtained by squaring the tension tensor as

$$E^{\mathrm{i}}_{\alpha\beta} = \frac{1}{2}\left(\frac{\partial u^{\mathrm{i}}_{\alpha}}{\partial \xi_{\beta}} + \frac{\partial u^{\mathrm{i}}_{\beta}}{\partial \xi_{\alpha}} + \frac{\partial u^{\mathrm{i}}_{\lambda}}{\partial \xi_{\alpha}}\frac{\partial u^{\mathrm{i}}_{\lambda}}{\partial \xi_{\beta}}\right), \tag{4}$$

$$E^{\mathrm{f}}_{\alpha\beta} = \frac{1}{2}\left(\frac{\partial u^{\mathrm{f}}_{\alpha}}{\partial \xi_{\beta}} + \frac{\partial u^{\mathrm{f}}_{\beta}}{\partial \xi_{\alpha}} + \frac{\partial u^{\mathrm{f}}_{\lambda}}{\partial \xi_{\alpha}}\frac{\partial u^{\mathrm{f}}_{\lambda}}{\partial \xi_{\beta}}\right), \tag{5}$$

where the repeated subscript indicates the sum, if not specified. Assuming that the superposed seismic wave perturbation is infinitesimal, the deformation increment caused by seismic wave perturbation can be expressed as

$$E_{\alpha\beta} = \frac{1}{2}\left(\frac{\partial u_{\alpha}}{\partial \xi_{\beta}} + \frac{\partial u_{\beta}}{\partial \xi_{\alpha}} + \frac{\partial u^{\mathrm{i}}_{\lambda}}{\partial \xi_{\alpha}}\frac{\partial u_{\lambda}}{\partial \xi_{\beta}} + \frac{\partial u^{\mathrm{i}}_{\lambda}}{\partial \xi_{\beta}}\frac{\partial u_{\lambda}}{\partial \xi_{\alpha}}\right). \tag{6}$$

The Kirchhoff stress increment caused by seismic wave perturbation in the initial state is

$$T_{JK} = T^{\mathrm{f}}_{JK} - T^{\mathrm{i}}_{JK}. \tag{7}$$

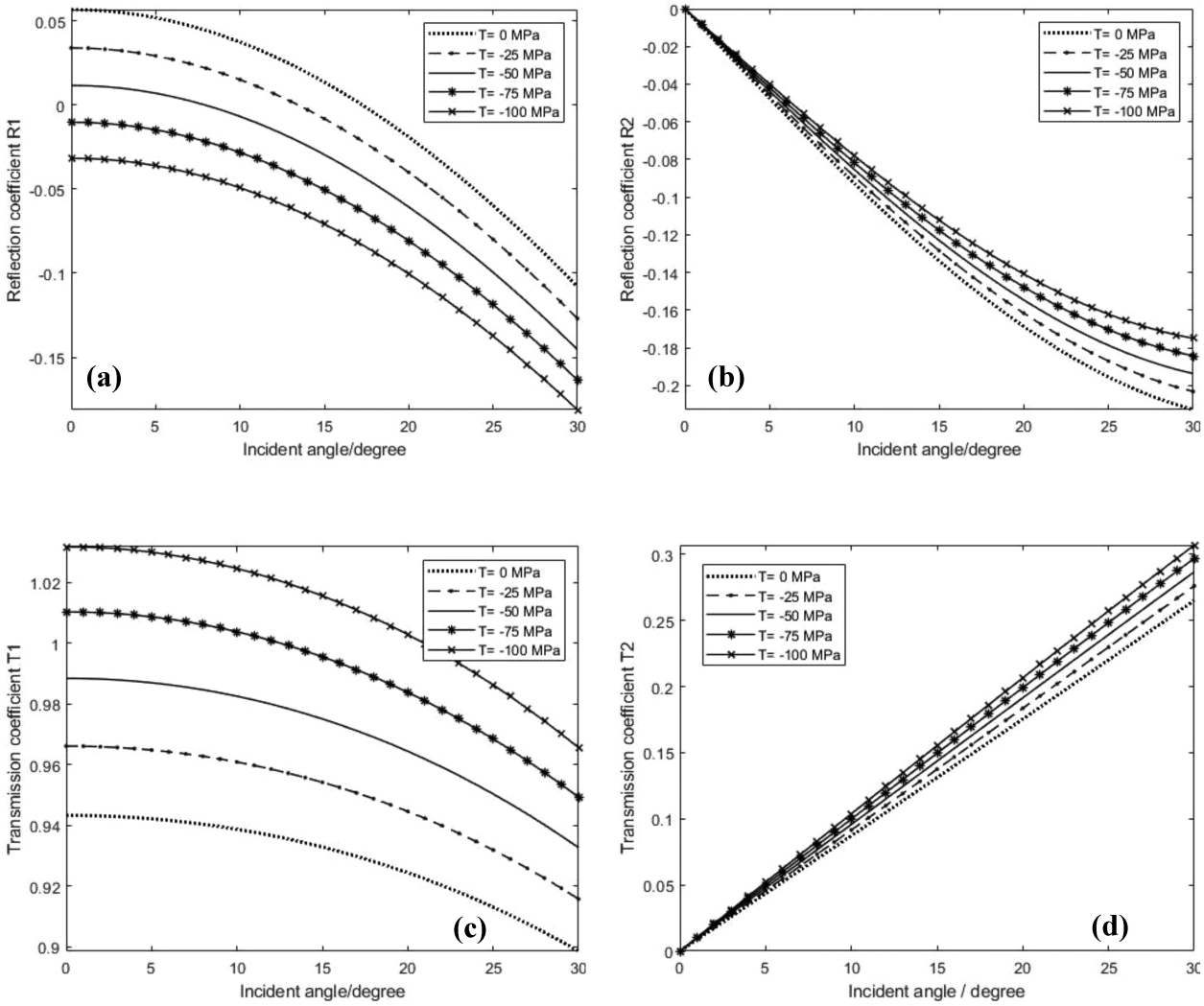

Figure 5. The seismic reflection coefficients and transmission coefficients at the interface between dry Berea1 sandstone and dry Portland sandstone under normal *in situ* stress. The dotted, dashed, solid, star marked and cross marked lines denote unstressed state, −25, −50, −75 and −100 MPa in rocks, respectively. (a) Reflection coefficient of *P* wave, (b) reflection coefficient of *SV* wave, (c) transmission coefficient of *P* wave and (d) transmission coefficient of *SV* wave.

For hyperelastic rock, the internal energy per unit mass of the deformed rock is W, which obeys the law of balance of energy. Therefore, the constitutive equation of hyperelastic rock can be built from the assumed internal energy function. The internal energy function (Pao *et al.* 1984) can be expanded as

$$\rho^0 W(E) = \frac{1}{2} c_{\alpha\beta\gamma\delta} E_{\alpha\beta} E_{\gamma\delta} + \frac{1}{6} c_{\alpha\beta\gamma\delta\varepsilon\eta} E_{\alpha\beta} E_{\gamma\delta} E_{\varepsilon\eta} + \cdots, \tag{8}$$

where $c_{\alpha\beta\gamma\delta}$ denotes the second-order elastic modulus and $c_{\alpha\beta\gamma\delta\varepsilon\eta}$ denotes the third-order elastic modulus. For isotropic rocks, if Voigt's notation is adopted to contract the indices of $c_{\alpha\beta\gamma\delta}$ and $c_{\alpha\beta\gamma\delta\varepsilon\eta}(11 \to 1, 22 \to 2, 33 \to 3, 23 \to 4, 13 \to 5, 12 \to 6)$, the independent components of second-order elastic modulus c_{ij} are $c_{11} = \lambda + 2\mu$, $c_{12} = \lambda + 2\mu$ and $c_{44} = \mu$; the independent components of third-order elastic modulus c_{ijk} are $c_{111} = 2A + 6B + 2C$, $c_{123} = 2C$ and $c_{112} = 2B + 2C$. Relationship between respective components of second-order elastic modulus and third-order elastic modulus can be found in Pao *et al* (1984) and Rasolofosaon (1998).

Ignoring the higher order terms in the equation, the rock constitutive equations can be obtained as

$$T^{\mathrm{i}}_{\alpha\beta} = c_{\alpha\beta\gamma\delta} E^{\mathrm{i}}_{\gamma\delta} + \frac{1}{2} c_{\alpha\beta\gamma\delta\varepsilon\eta} E^{\mathrm{i}}_{\gamma\delta} E^{\mathrm{i}}_{\varepsilon\eta}, \tag{9}$$

$$T^{\mathrm{f}}_{\alpha\beta} = c_{\alpha\beta\gamma\delta} E^{\mathrm{f}}_{\gamma\delta} + \frac{1}{2} c_{\alpha\beta\gamma\delta\varepsilon\eta} E^{\mathrm{f}}_{\gamma\delta} E^{\mathrm{f}}_{\varepsilon\eta}. \tag{10}$$

Substituting eqs (9) and (10) into eq. (7), the rock constitutive equation can be expressed as

$$T_{\alpha\beta} = c_{\alpha\beta\gamma\delta} E_{\gamma\delta} + c_{\alpha\beta\gamma\delta\varepsilon\eta} e^{\mathrm{i}}_{\gamma\delta} e_{\varepsilon\eta}, \tag{11}$$

where e^{i} and e are infinitesimal strains, $e_{\alpha\beta} = \frac{1}{2}\left(\frac{\partial u_\alpha}{\partial \xi_\beta} + \frac{\partial u_\beta}{\partial \xi_\alpha}\right)$.

Substituting eq. (6) into eq. (11), according to the relationship between T_{IJ} and $T_{\alpha\beta}$, the stress increment in the initial coordinate system can be obtained as,

$$T_{IJ} = \delta_{I\alpha}\delta_{J\beta}\left[T_{\alpha\beta}\left(1 - \frac{\partial u^{\mathrm{i}}_\gamma}{\partial \xi_\gamma}\right) + T_{\alpha\gamma}\frac{\partial u^{\mathrm{i}}_\beta}{\partial \xi_\gamma} + T_{\beta\gamma}\frac{\partial u^{\mathrm{i}}_\alpha}{\partial \xi_\gamma}\right]. \tag{12}$$

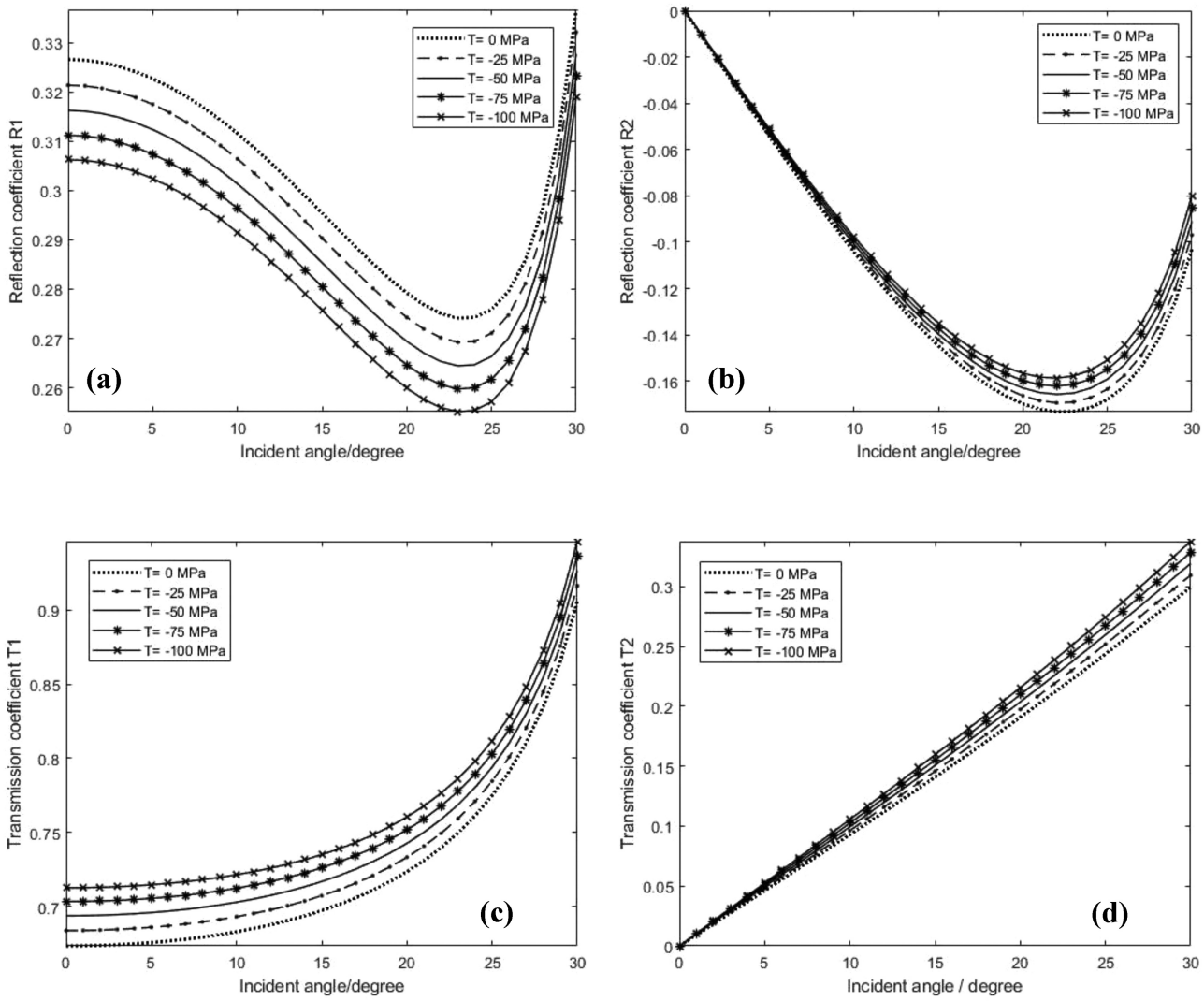

Figure 6. The seismic reflection coefficients and transmission coefficients at the interface between dry Berea1 sandstone and dry Indiana limestone under normal *in situ* stress. The dotted, dashed, solid, star marked and cross marked lines denote unstressed state, −25, −50, −75 and −100 MPa in rocks, respectively. (a) Reflection coefficient of *P* wave, (b) reflection coefficient of *SV* wave, (c) transmission coefficient of *P* wave and (d) transmission coefficient of *SV* wave.

Eq. (12) can be further described as

$$T_{IJ}=C_{IJKL}\frac{\partial u_K}{\partial X_L}, \tag{13}$$

where

$$C_{IJKL} = c_{IJKL}(1-e^{i}_{NN}) + c_{IJKLMN}e^{i}_{MN} + c_{MJKL}\frac{\partial u^{i}_{I}}{\partial X_M} + c_{IMKL}\frac{\partial u^{i}_{J}}{\partial X_M} + c_{IJML}\frac{\partial u^{i}_{K}}{\partial X_M} + c_{IJKM}\frac{\partial u^{i}_{L}}{\partial X_M}. \tag{14}$$

The pre-deformation from the natural state to the initial state is static, and the Cauchy stress tensor and Kirchhoff stress tensor must meet the equilibrium equation

$$\frac{\partial t^{i}_{JK}}{\partial X_K} = 0. \tag{15}$$

And the motion equation of a rock particle from the initial state to the final state is

$$\frac{\partial}{\partial X_K}T^{f}_{KJ} + T^{f}_{KL}\frac{\partial u_J}{\partial X_L} = \rho^{i}\frac{\partial^2 u_J}{\partial t^2}. \tag{16}$$

Subtracting eq. (15) from eq. (16), and ignoring high-order small terms, we can get a rock particle motion equation described by the displacement increment caused by the seismic wave perturbation

$$\frac{\partial}{\partial X_J}\left[T_{IJ} + t^{i}_{JK}\frac{\partial u_I}{\partial X_K}\right] = \rho^{i}\frac{\partial^2 u_I}{\partial t^2}. \tag{17}$$

Only two assumptions have been made in the derivation. The pre-deformation is static, and the seismic wave perturbations are infinitesimal. Therefore, the motion equation (17) can be applied to pre-deformed, elastic and inelastic rocks (Tian & Hu 2010).

Substituting eq. (13) into eq. (17), the motion equation of a rock particle caused by seismic wave perturbation, that is the solid

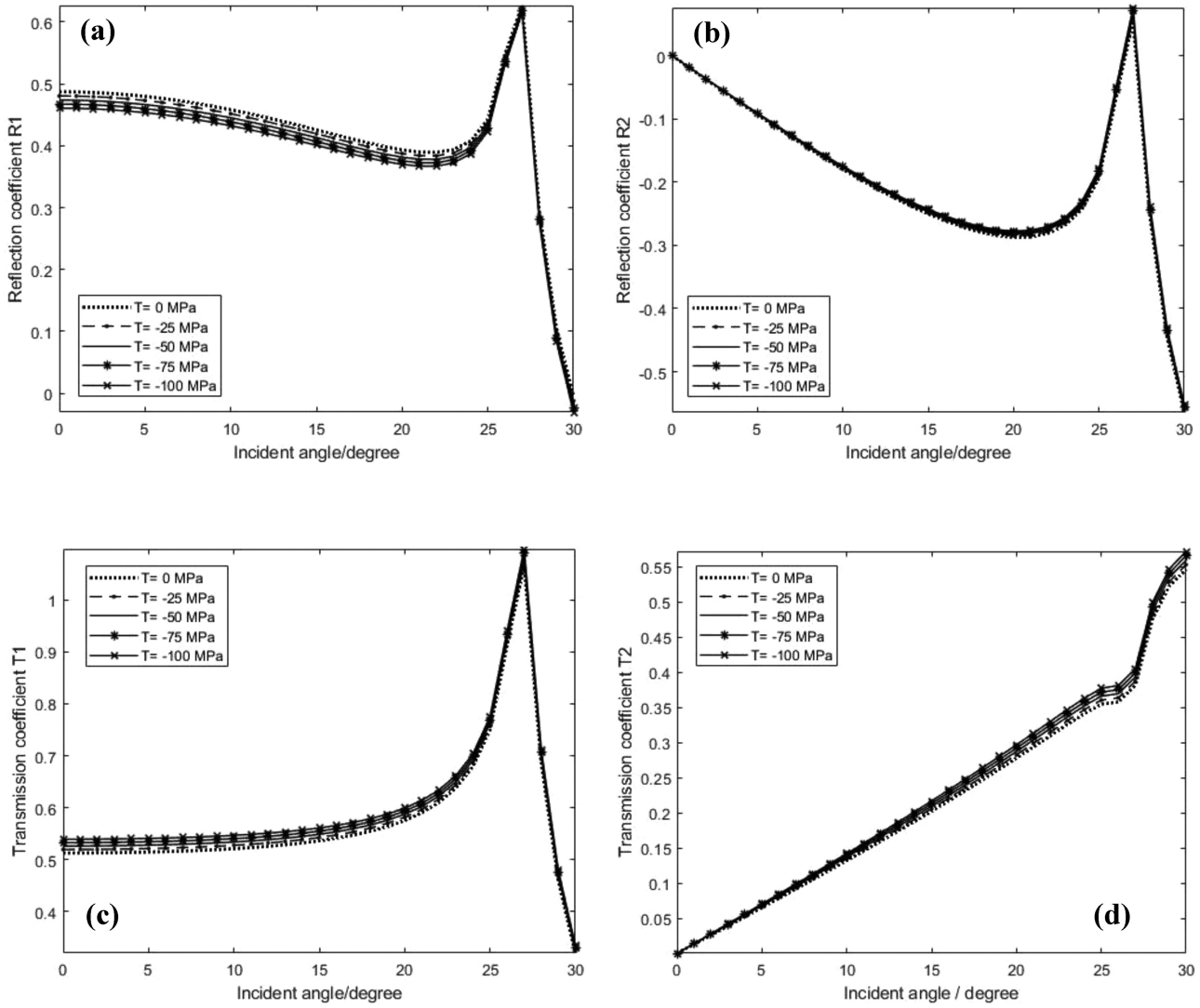

Figure 7. The seismic reflection coefficients and transmission coefficients at the interface between dry Berea1 sandstone and dry granite under normal *in situ* stress. The dotted, dashed, solid, star marked and cross marked lines denote unstressed state, −25, −50, −75 and −100 MPa in rocks, respectively. (a) Reflection coefficient of *P* wave, (b) reflection coefficient of *SV* wave, (c) transmission coefficient of *P* wave and (d) transmission coefficient of *SV* wave.

acoustoelastic equation, can be expressed as

$$\frac{\partial}{\partial X_J}\left[(\delta_{IK}t^{\mathrm{i}}_{JL}+C_{IJKL})\frac{\partial u_K}{\partial X_L}\right]=\rho^{\mathrm{i}}\frac{\partial^2 u_I}{\partial t^2}. \tag{18}$$

Assuming that the medium is homogeneously deformed, the acoustoelastic equation can be reduced to

$$B_{IJKL}\frac{\partial^2 u_K}{\partial X_J \partial X_L}=\rho^{\mathrm{i}}\frac{\partial^2 u_I}{\partial t^2}, \tag{19}$$

in which

$$B_{IJKL}=\delta_{IK}t^{\mathrm{i}}_{JL}+C_{IJKL}. \tag{20}$$

Under the assumption that the seismic waves are plane waves. The displacement equation of seismic plane wave in the initial coordinate system is

$$u_k=aP_k\exp\left[\mathrm{i}K(N_JX_J-Vt)\right], \tag{21}$$

where a, V, $K$and P_k respectively denote the amplitude, velocity, wave number and polarization vector. Substitute eq. (21) into eq. (19), then we can obtain a system of equations for the polarization vector P_k,

$$(B_{IJKL}m_Jm_L-\rho^{\mathrm{i}}\delta_{IK})P_K=0. \tag{22}$$

The polarization vector has non-zero solutions, and the characteristic equation satisfies

$$|B_{IJKL}m_Jm_L-\rho^{\mathrm{i}}\delta_{IK}|=0, \tag{23}$$

in which m_J and m_L can be interpreted as seismic wave slowness. The seismic wave slowness in different propagation directions can be obtained according to the above equation.

Normal *in situ* stress

Normal *in situ* stress is generated from the gravity of the overlying strata. Hence, it can be obtained by integrating the density of the strata obtained from well logging data. Normal initial stress can be calculated by the following formula (Abdideh & Moghimzadeh 2019):

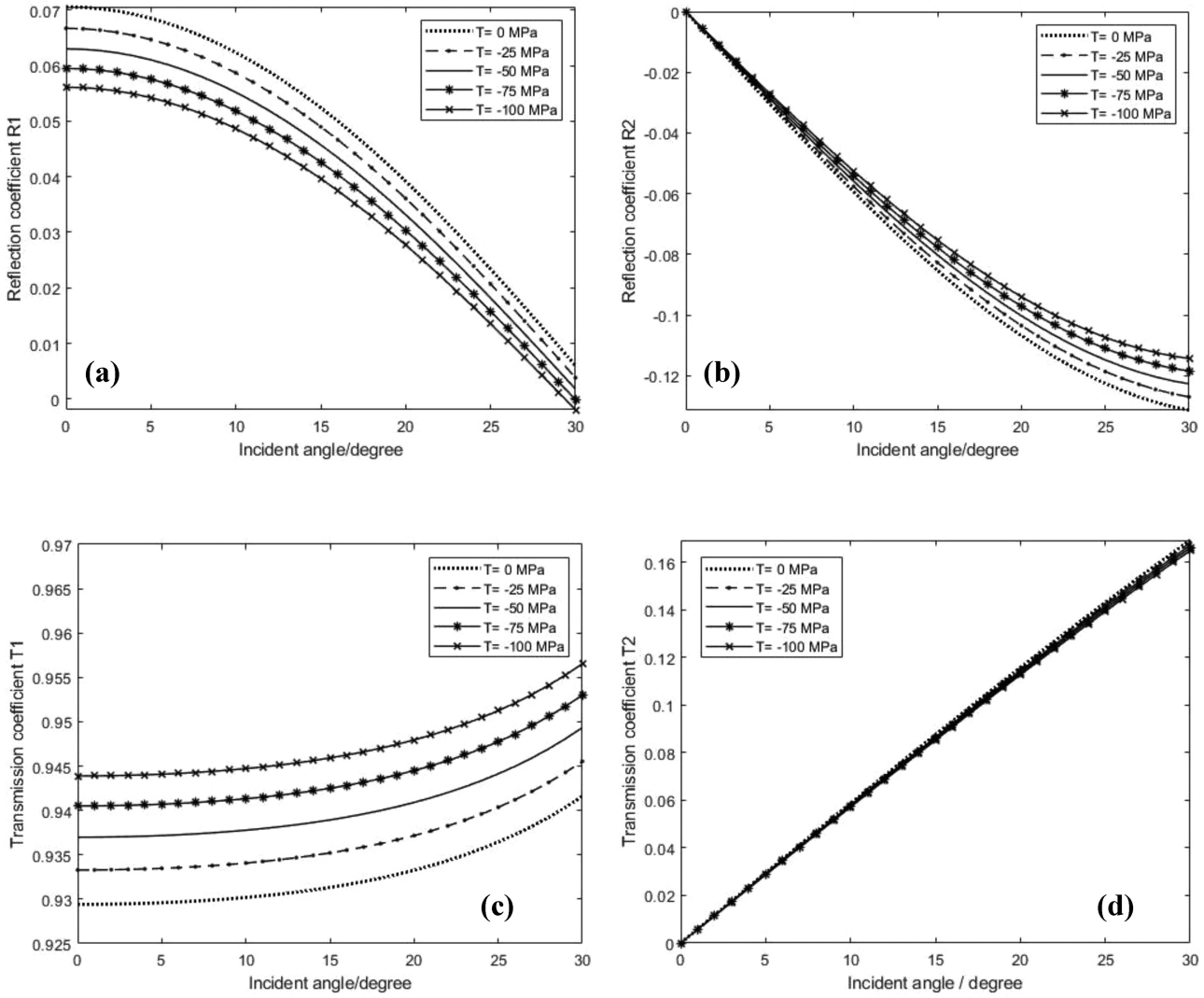

Figure 8. The seismic reflection coefficients and transmission coefficients at the interface between saturated Berea1 sandstone and saturated Berea2 sandstone under normal *in situ* stress. The dotted, dashed, solid, star marked and cross marked lines denote unstressed state, −25, −50, −75 and −100 MPa in rocks, respectively. (a) Reflection coefficient of *P* wave, (b) reflection coefficient of *SV* wave, (c) transmission coefficient of *P* wave and (d) transmission coefficient of *SV* wave.

$$t^0 = \rho_f g z_f + g \int_{z_w}^{z} \rho_s(z)\mathrm{d}z, \tag{24}$$

where ρ_f is the density of the sea water for offshore drilling; g is gravity acceleration; z_f is the depth of water, for onshore drilling $z_f = 0$; z is the depth from the sea level to the seabed; and $\rho_s(z)$ is the stratum bulk density expressed as a function of depth.

Reflectivity and transmissivity equations

At the solid–solid interface, the Cauchy stress values are equal, so the first Piola–Kirchhoff stress tensor can be expressed as (Degtyar 1998)

$$\sigma_{IJ} = C_{IJKL} e_{KL} + u_{I,K} t^0_{KJ}. \tag{25}$$

Assuming that the transverse principal strains e_{11} and e_{22} are equal. When the seismic *P* wave propagates to the interface between two different stressed strata, it is converted into two kinds of reflected wave and two kinds of transmitted wave in the upper and lower strata in the *X*–*Z* plane, respectively, as shown in Fig. 2.

The displacement u and the normal stress at the solid–solid interface are continuous. Thus, the boundary condition (Degtyar 1998) at the interface is

$$\left(u_I^0 + \sum_{\alpha=1}^{3} u_I^\alpha\right)_{z=0} = \left(\sum_{\alpha=4}^{6} u_I^\alpha\right)_{z=0}, \tag{26}$$

$$\left(\sigma_{I3}^0 + \sum_{\alpha=1}^{3} \sigma_{I3}^\alpha\right)_{z=0} = \left(\sum_{\alpha=4}^{6} \sigma_{I3}^\alpha\right)_{z=0}, I = 1, 2, 3. \tag{27}$$

Substitute eqs (21) and (25) into the boundary condition. According to Snell's law, we utilize the relationship between velocity and slowness to derive the reflection coefficient and transmission coefficient equations as

$$\begin{bmatrix} P_1^1 & P_1^2 & P_1^3 & -P_1^4 & -P_1^5 & -P_1^6 \\ P_2^1 & P_2^2 & P_2^3 & -P_2^4 & -P_2^5 & -P_2^6 \\ P_3^1 & P_3^2 & P_3^3 & -P_3^4 & -P_3^5 & -P_3^6 \\ Y_{41} & Y_{42} & Y_{43} & Y_{44} & Y_{45} & Y_{46} \\ Y_{51} & Y_{52} & Y_{53} & Y_{54} & Y_{55} & Y_{56} \\ Y_{61} & Y_{62} & Y_{63} & Y_{64} & Y_{65} & Y_{66} \end{bmatrix} \begin{bmatrix} R_1 \\ R_2 \\ R_3 \\ T_1 \\ T_2 \\ T_3 \end{bmatrix} = \begin{bmatrix} -P_1^0 \\ -P_2^0 \\ -P_3^0 \\ Z_1 \\ Z_2 \\ Z_3 \end{bmatrix}, \tag{28}$$

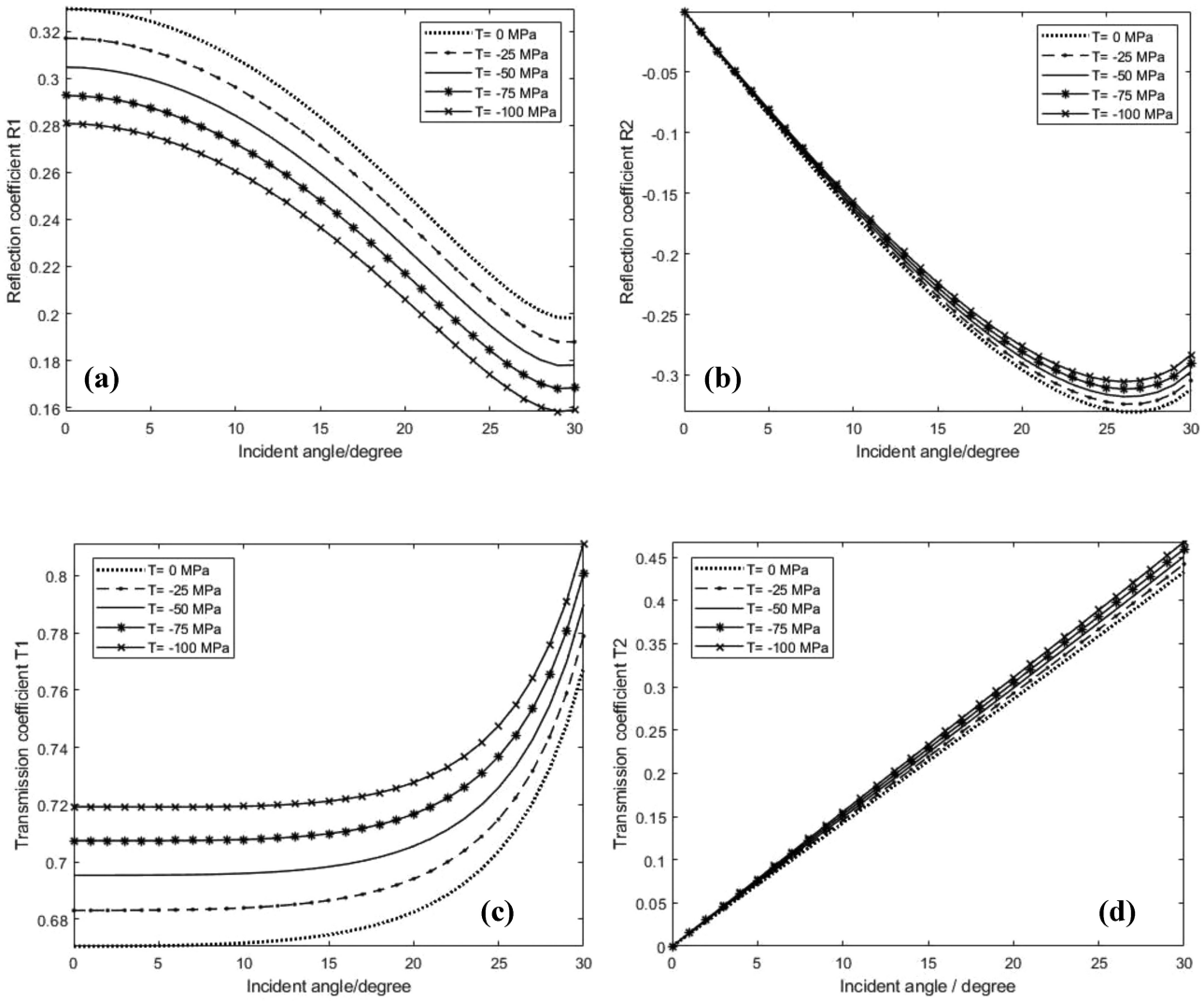

Figure 9. The seismic reflection coefficients and transmission coefficients at the interface between saturated Berea1 sandstone and saturated tight rock under normal *in situ* stress. The dotted, dashed, solid, star marked and cross marked lines denote unstressed state, −25, −50, −75 and −100 MPa in rocks, respectively. (a) Reflection coefficient of *P* wave, (b) reflection coefficient of *SV* wave, (c) transmission coefficient of *P* wave and (d) transmission coefficient of *SV* wave.

where

$$
\begin{aligned}
&Y_{41}=C^{\mathrm{up}}_{13KL}P^1_Km^1_L+P^1_1m^1_Kt^0_{K3},\ Y_{42}=C^{\mathrm{up}}_{13KL}P^2_Km^2_L+P^2_1m^2_Kt^0_{K3},\\
&Y_{43}=C^{\mathrm{up}}_{13KL}P^3_Km^3_L+P^3_1m^3_Kt^0_{K3},\ Y_{44}=-C^{\mathrm{low}}_{13KL}P^4_Km^4_L-P^4_1m^4_Kt^0_{K3},\\
&Y_{45}=-C^{\mathrm{low}}_{13KL}P^5_Km^5_L-P^5_1m^5_Kt^0_{K3},\ Y_{46}=-C^{\mathrm{low}}_{13KL}P^6_Km^6_L-P^6_1m^6_Kt^0_{K3},\\
&Y_{51}=C^{\mathrm{up}}_{23KL}P^1_Km^1_L+P^1_2m^1_Kt^0_{K3},\ Y_{52}=C^{\mathrm{up}}_{23KL}P^2_Km^2_L+P^2_2m^2_Kt^0_{K3},\\
&Y_{53}=C^{\mathrm{up}}_{23KL}P^3_Km^3_L+P^3_2m^3_Kt^0_{K3},\ Y_{54}=-C^{\mathrm{low}}_{23KL}P^4_Km^4_L-P^4_2m^4_Kt^0_{K3},\\
&Y_{55}=-C^{\mathrm{low}}_{23KL}P^5_Km^5_L-P^5_2m^5_Kt^0_{K3},\ Y_{56}=-C^{\mathrm{low}}_{23KL}P^6_Km^6_L-P^6_2m^6_Kt^0_{K3},\\
&Y_{61}=C^{\mathrm{up}}_{33KL}P^1_Km^1_L+P^1_3m^1_Kt^0_{K3},\ Y_{62}=C^{\mathrm{up}}_{33KL}P^2_Km^2_L+P^2_3m^2_Kt^0_{K3},\\
&Y_{63}=C^{\mathrm{up}}_{33KL}P^3_Km^3_L+P^3_3m^3_Kt^0_{K3},\ Y_{64}=-C^{\mathrm{low}}_{33KL}P^4_Km^4_L-P^4_3m^4_Kt^0_{K3},\\
&Y_{65}=-C^{\mathrm{low}}_{33KL}P^5_Km^5_L-P^5_3m^5_Kt^0_{K3},\ Y_{66}=-C^{\mathrm{low}}_{33KL}P^6_Km^6_L-P^6_3m^6_Kt^0_{K3},\\
&Z_1=-C^{\mathrm{up}}_{13KL}P^0_Km^0_L-P^0_1m^0_Kt^0_{K3},\ Z_2=-C^{\mathrm{up}}_{23KL}P^0_Km^0_L-P^0_2m^0_Kt^0_{K3},\\
&Z_3=-C^{\mathrm{up}}_{33KL}P^0_Km^0_L-P^0_3m^0_Kt^0_{K3}.
\end{aligned}
\tag{29}
$$

According to Snell's law, the projections of the slowness vectors along the interface m^α_1 ($\alpha=0,1,2,3,4,5,6$) are equal to m^0_1, which is already known. The unknown m^α_3 can be precisely determined from the eq. (23). Then, the polarization vector corresponding to each slowness can be obtained by substituting slowness into eq. (24). In this case, no birefringence occurs in the *X*–*Z* plane, so the reflection coefficient R_3 and transmission coefficient T_3 of *SH* wave vanish.

NUMERICAL ANALYSIS

Various rocks, such as Castalegeta sandstone, tight rock (porosity≈1.9 per cent), limestone and granite, are used to construct stratigraphic models to obtain corresponding seismic reflection and transmission coefficients. Parameters of the rocks used in stratigraphic models (Wang 2002; Prioul *et al.* 2004; Winkler & Larry 2004; Liu *et al.* 2012) are shown in Table 1. Two kinds of model are used in our analysis: the interface between two formations which have different lithology and the same saturated state, and the interface between two formations which have same lithology and the different saturated state. By observing the seismic reflection and transmission coefficients of the above two models, the effect of *in situ* stress under different models is preliminarily determined.

First, we discuss the effect of *in situ* stress on the reflection and transmission at the interface between two formations which

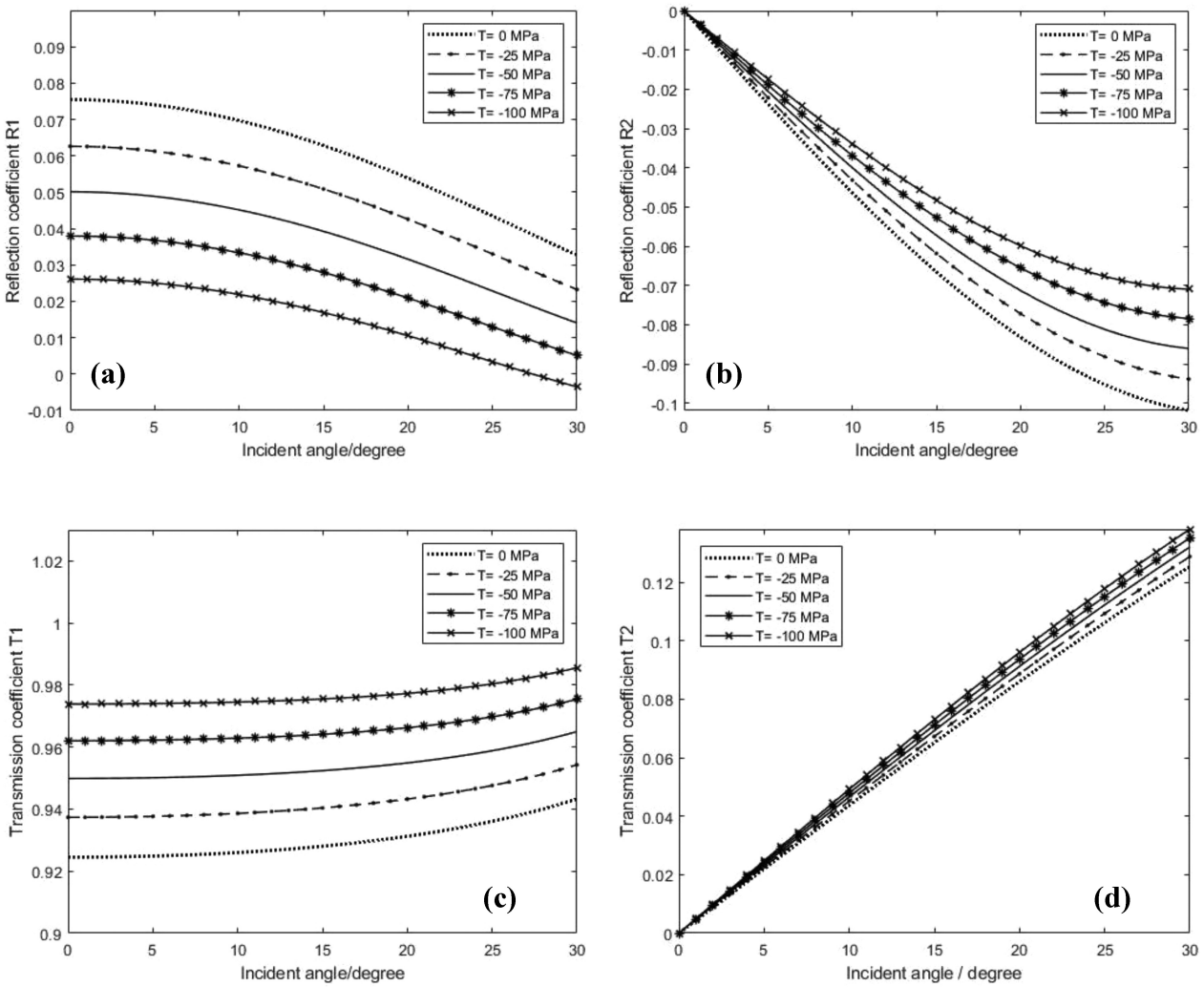

Figure 10. The seismic reflection coefficients and transmission coefficients at the interface between saturated Berea1 sandstone and saturated Portland sandstone under normal *in situ* stress. The dotted, dashed, solid, star marked and cross marked lines denote unstressed state, −25, −50, −75 and −100 MPa in rocks, respectively. (a) Reflection coefficient of *P* wave, (b) reflection coefficient of *SV* wave, (c) transmission coefficient of *P* wave and (d) transmission coefficient of *SV* wave.

have different lithology and the same saturated state. Figs 3(a)–(d) respectively show the *P*-wave reflection coefficient, *SV*-wave reflection coefficient, *P*-wave transmission coefficient and *SV*-wave transmission coefficient at the interface between dry Berea1 sandstone (upper layer) and dry Berea2 sandstone (lower layer). With the continuous increase of the normal *in situ* stress caused by the increasing burial depth of the formation, the values of the reflection coefficients of the *P* wave and *SV* wave gradually decrease, while the transmission coefficients of the *P* wave and *SV* wave gradually increase. The *SV*-wave reflection coefficient is negative. This phenomenon is consistent with that shown from Figs 4 to 7 at low incident angle (lower than critical angle). However, the transmission coefficients of the *P* wave and *SV* wave are almost not affected by the increase of the stress at the interface between dry Berea1 sandstone (upper layer) and tight rock (lower layer), as shown in Fig. 4, and at the interface dry Berea1 sandstone (upper layer) and granite (lower layer), as shown in Fig. 7.

Similar analyses were implemented on saturated rocks. Fig. 8 shows the seismic reflection and transmission coefficients at the interface between saturated Berea1 sandstone (upper layer) and saturated Berea2 sandstone (lower layer). The *in situ* stress has little effect on the reflection and transmission coefficient of *SV* wave at low incident angle. Compared with the results shown in Fig. 3, when the rock is filled with fluid, the effect of *in situ* stress on the *P*-wave transmission coefficient remains nearly unchanged, while the effect of stress on the *SV*-wave transmission coefficient decreases. Comparison between Figs 9 and 4 or comparison between Figs 10 and 5 shows when the dry rock is filled with fluid, the effect of *in situ* stress on the reflection and transmission coefficient of *P* wave remains the same as before. Nevertheless, the presence of fluid increases the critical incident angle (shown in Figs 9 and 4). Seismic reflection and transmission coefficients of *P* wave are still sensitive to *in situ* stress. However, the reflection coefficient and transmission coefficient of *SV* wave become very insensitive to *in situ* stress. According to the results shown in Figs 11 and 6, it can be found that the stress has a great effect on the *P*-wave reflection coefficient and the critical angle increase when the rock is filled with fluid. While the effect of stress on the *SV*-wave reflection coefficient, *P*-wave transmission coefficient and *SV*-wave transmission coefficient is significantly reduced, which is almost negligible.

We also make a discussion of the effect of *in situ* stress on the reflection and transmission at the interface between two formations

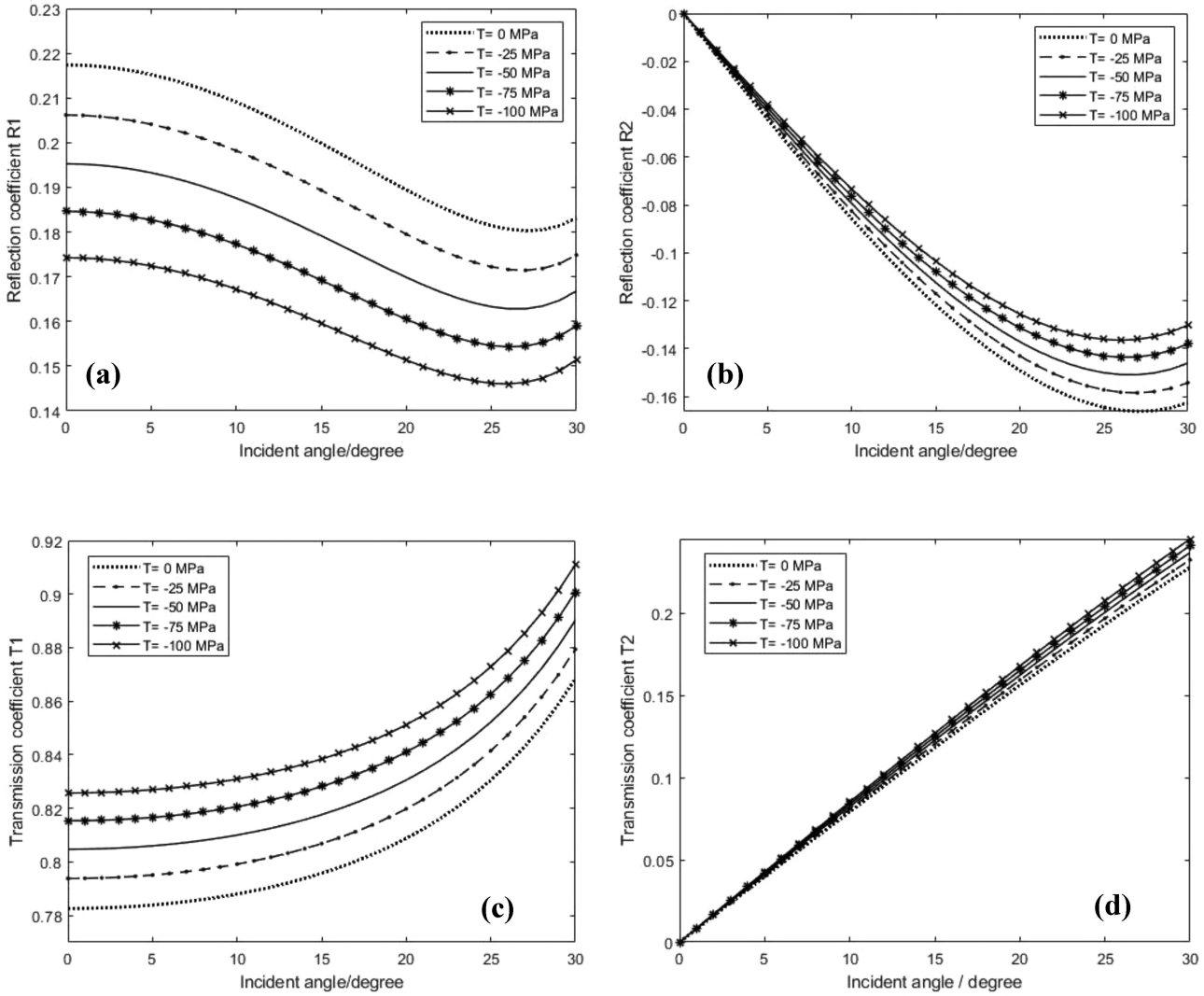

Figure 11. The seismic reflection coefficients and transmission coefficients at the interface between saturated Berea1 sandstone and saturated Indiana limestone under normal *in situ* stress. The dotted, dashed, solid, star marked and cross marked lines denote unstressed state, −25, −50, −75 and −100 MPa in rocks, respectively. (a) Reflection coefficient of *P* wave, (b) reflection coefficient of *SV* wave, (c) transmission coefficient of *P* wave and (d) transmission coefficient of *SV* wave.

with same lithology and different saturated state. This part is designed to analyse the effects of fluids on reflection and transmission at the interface of two stressed rocks. We set dry Portland sandstone as the upper layer and saturated Portland rock as the lower one. Figs 12(a)–(d) show the *P*-wave reflection coefficient, *SV*-wave reflection coefficient, *P*-wave transmission coefficient and *SV*-wave transmission coefficient at the interface of this model respectively. It is obvious that when the *in situ* stress increases, the reflection coefficient of *P* wave and *SV* wave and the transmission coefficient of *SV* increase gradually. However, the transmission coefficient of *P* wave decreases gradually with the increase of stress. The transmission coefficient of *SV* is negative and shows a good sensitivity to normal *in situ* stress in this model. The effect of normal stress on reflection and transmission at the interface between dry and saturated tight rock is investigated, as shown in Fig. 13. Because of the low porosity($\approx$ 1.9 per cent) of tight rock, the reflection coefficient of *P* wave, the transmission coefficient of *P* and *SV* wave are greatly small; the transmission coefficient of *P* wave is about 1. That means that the effect of the fluid on seismic reflection and transmission of tight rock is tiny, and all of the energy of incident *P* wave is almost transmitted, reflects little. We further use dry Indiana limestone as the upper layer and saturated Indiana limestone as the lower layer. The variation of reflection coefficient and transmission coefficient with the normal *in situ* stress as it is shown in Fig. 14. The reflection coefficient of both the absolute value of *P* wave and the *SV* wave increase with the increase of *in situ* stress. The transmission coefficient of *SV* wave is negative and very small, almost not affected by stress.

According to the results shown in Figs 12–14, the values of reflection coefficient and transmission coefficient of the Portland sandstone model, the tight rock model and the Indiana limestone model are very different. This phenomenon may be related to the difference of saturation, porosity and internal structure of the upper and lower formation. In spite of this, the variation trend of reflectivity, transmissivity and *in situ* stress sensitivity are quite similar. And the stress sensitivity of three models are very low. To sum

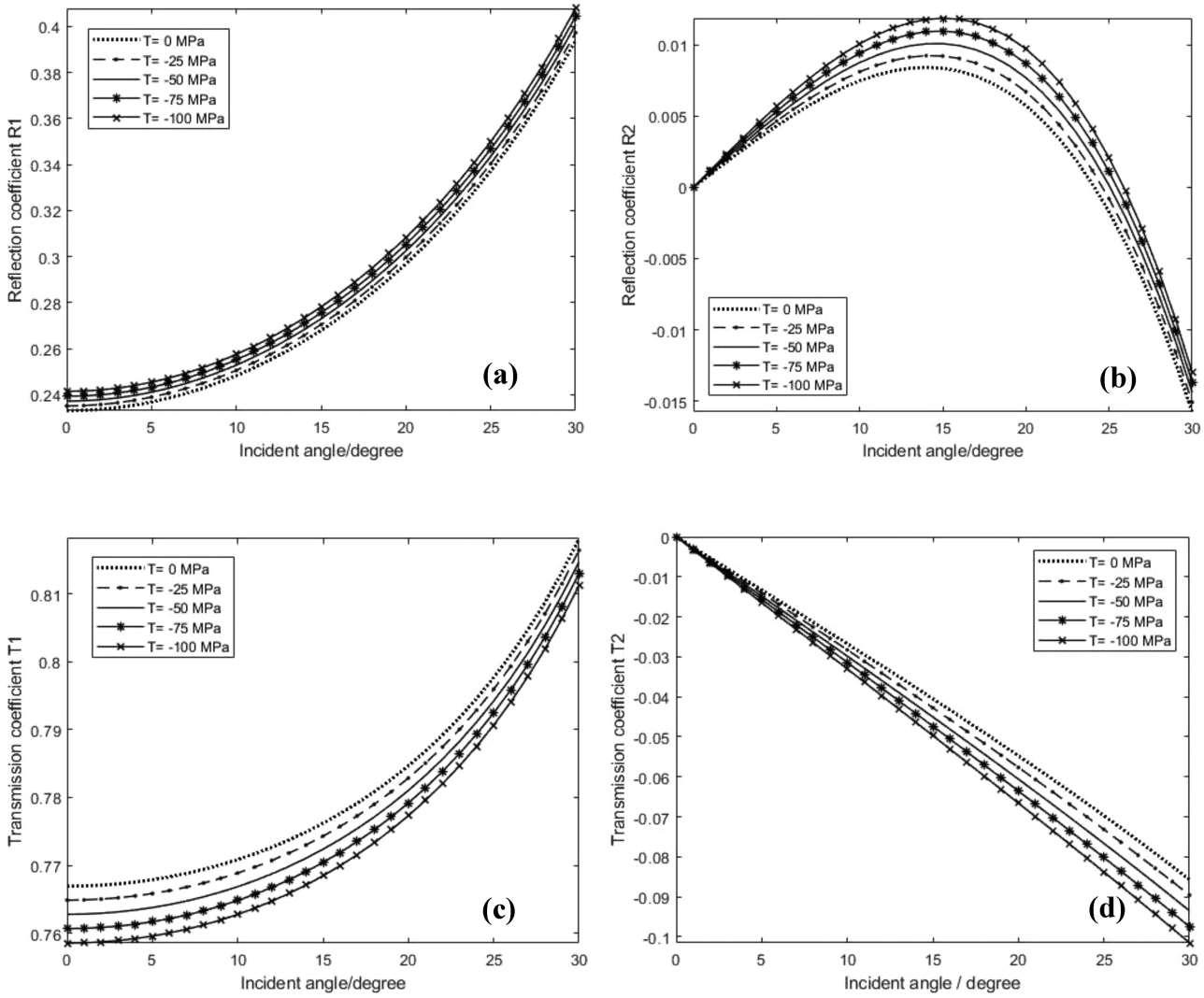

Figure 12. The seismic reflection coefficients and transmission coefficients at the interface between dry Portland sandstone and saturated Portland sandstone under normal *in situ* stress. The dotted, dashed, solid, star marked and cross marked lines denote unstressed state, −25, −50, −75 and −100 MPa in rocks, respectively. (a) Reflection coefficient of *P* wave, (b) reflection coefficient of *SV* wave, (c) transmission coefficient of *P* wave and (d) transmission coefficient of *SV* wave.

up, when the lower layer is sandstone, the critical incident angle decreases with the increase of normal stress; when the lower layer is limestone, the critical incident angle increases as normal stress increases; when the lower layer is tight rock or granite, the critical incident angle is invariable with the increase of normal stress. And the fluid of the rock creates the small impedance contrast between dry rock and saturated rock. The existence of the fluid has little influence on the behaviour of the normal stress.

FORMULA VERIFICATION

In this section, saturated Castlegate sandstone and saturated Berea3 sandstone are selected as the upper and lower medium respectively. This model will be used to verify the correctness of the reflectivity and transmissivity equations considering the effect of normal *in situ* stress. Fig. 15 shows the reflection coefficient and transmission coefficient at the interface of this model. The *in situ* stress has little influence on the *SV*-wave reflection coefficient, *P*-wave transmission coefficient and *SV*-wave transmission coefficient. The reflection coefficient of *P* wave decreases with the increase of stress at low incident angles, which is different from the partial results of the models used in previous sections. This indicates that the effect of stress on the reflection and transmission coefficients is closely related to the properties of rocks as well, such as third-order elastic modulus, seismic velocity, density and saturation state.

The solid curve in Fig. 15 represents the calculated result of eq. (28) when the normal *in situ* stress is zero, and the curve marked with hollow circle represents the calculated result of Zoeppritz equation. We can find that the solid and the red hollow circle are identical. In other words, when the *in situ* stress becomes zero, eq. (28) can be degenerated to the Zoeppritz equation, which preliminarily verifies the correctness of eq. (28) we proposed. From Figs 3, 5, 8 and 10, we can find that the critical incident angles of the reflection coefficient or transmission coefficient equation at the interface between Beare1 sandstone (dry or saturated, upper layer) and Berea2 or Portland sandstone (dry, saturated, lower layer) decrease continuously with the increase of stress. This is consistent with the previous conclusion that the critical incident angles

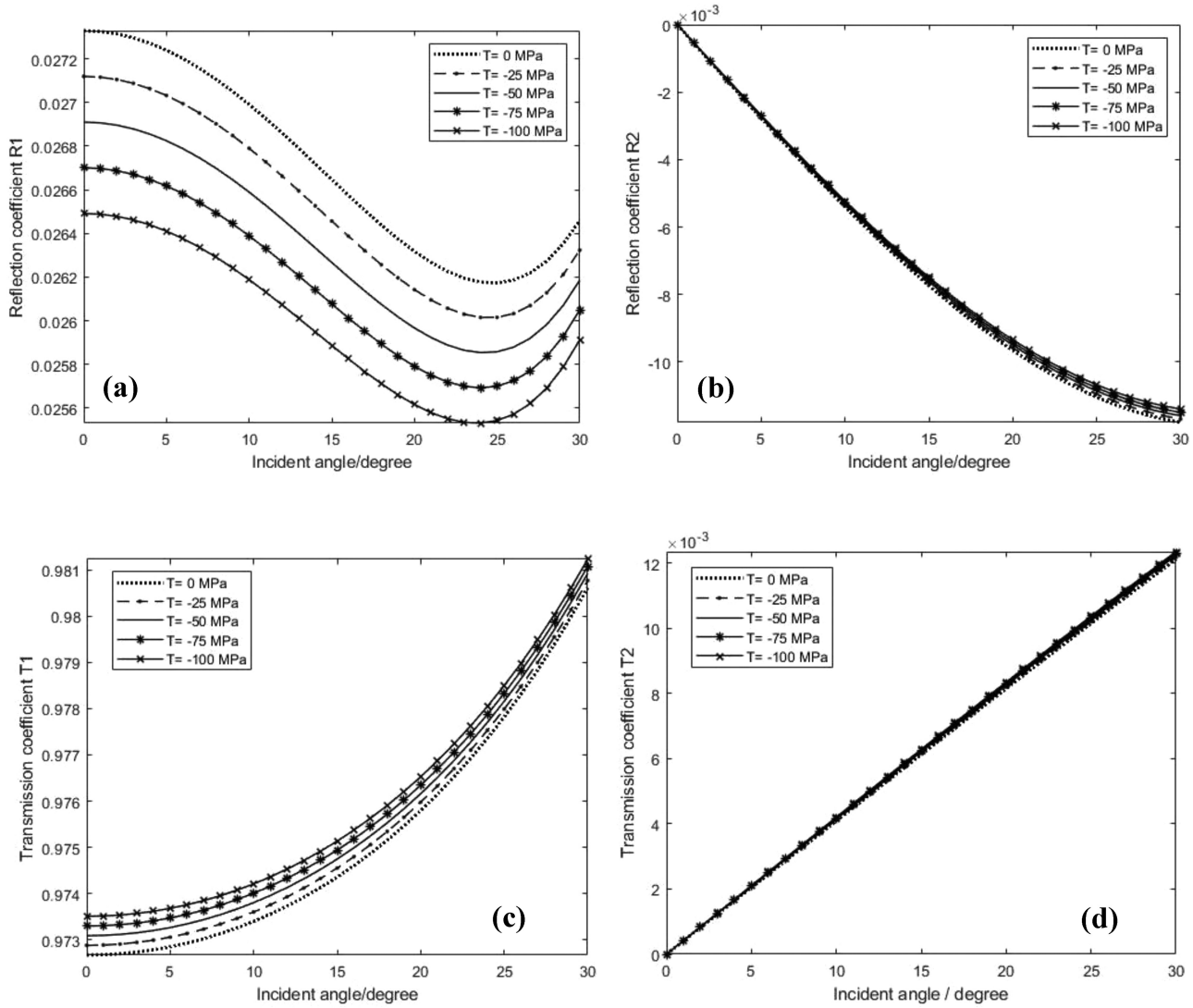

Figure 13. The seismic reflection coefficients and transmission coefficients at the interface between dry tight rock and saturated tight rock under normal *in situ* stress. The dotted, dashed, solid, star marked and cross marked lines denote unstressed state, −25, −50, −75 and −100 MPa in rocks, respectively. (a) Reflection coefficient of *P* wave, (b) reflection coefficient of *SV* wave, (c) transmission coefficient of *P* wave and (d) transmission coefficient of *SV* wave.

of the energy reflection and transmission coefficients decrease with the increase of stress, which further demonstrates the accuracy of eq. (28).

DISCUSSION

Based on the main assumption of planar seismic wave and isotropic medium, the exact seismic amplitude reflectivity and transmissivity equations under the vertical normal *in situ* stress at the horizontal interface were derived by combining the acoustoelastic theory and elastic wave dynamics.

Through analysing different rock models, the effect of stress on the reflection and transmission coefficients at the interface between two formations with different lithology and saturated state was obtained. The stress mainly affects the amplitude and critical incident angle of reflectivity and transmissivity. The upper layer was given as sandstone; the critical incident angle decreased when the lower layer was sandstone (dry or saturated), was invariable when the lower layer was tight or granite rock (dry or saturated) and increased when the lower layer was limestone (dry or saturated). In all rock models, the *P*-wave reflectivity and *SV*-wave reflectivity (absolute values) decreased and the *P* wave increased with the increase of stress. The *SV*-wave transmissivity was insensitive to stress.

Previous studies mainly focused on seismic amplitude reflection and transmission coefficients in stress-free state, or seismic energy reflection and transmission under transverse stress at the rock interface, without considering the effect of the vertical normal stress. In fact, the underground rocks always are subjected to normal *in situ* stress. The proposed equation is expected to lay the foundation for seismic prediction of *in situ* stress.

However, the hypothesis of this study will cause some inherent limitations of the exact equation. The main limitation is that the rock is assumed to be isotropic, without considering the influence of rock porosity on seismic wave propagation. Therefore, we can find that the reflection coefficient increases or decreases almost linearly with the increase of stress. In addition, because of the assumption that saturated rocks are regarded as equivalent isotropic rocks, we can find that the effect of stress on the reflection coefficient is not very different for dry and saturated rocks of the same lithology.

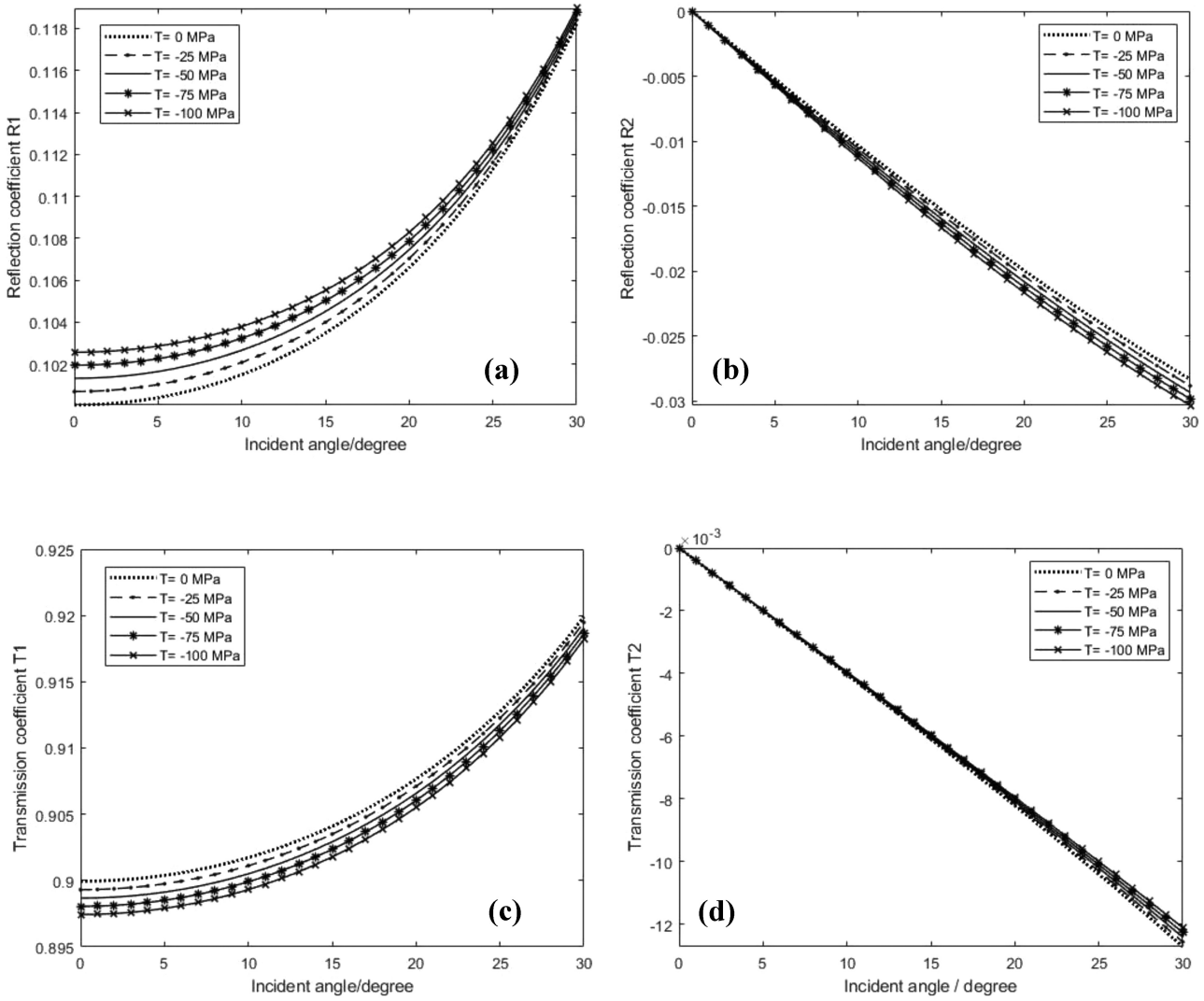

Figure 14. The seismic reflection coefficients and transmission coefficients at the interface between dry Indiana limestone and saturated Indiana limestone under normal *in situ* stress. The dotted, dashed, solid, star marked and cross marked lines denote unstressed state, −25, −50, −75 and −100 MPa in rocks, respectively. (a) Reflection coefficient of *P* wave, (b) reflection coefficient of *SV* wave, (c) transmission coefficient of *P* wave and (d) transmission coefficient of *SV* wave.

Therefore, it is difficult to analyse the detailed influence of fluid in stressed rock on seismic reflection by the equation proposed in this paper. In fact, due to the existence of pores, the reflection coefficient increases almost linearly with the increase of stress at low stress. Then, the growth rate of the reflection coefficient becomes slow. Finally, the reflection coefficient tends to be stable gradually with the increase of stress due to the closure of rock pores. Therefore, the equation presented in this paper has good stability and accuracy only when the stress is low.

In the future work, the reflection coefficient equation considering rock pore and fluid should be constructed to solve the above limitations, which can describe the reflection and transmission of seismic wave with the effect of *in situ* stress more accurately.

CONCLUSIONS

According to the results of the above comparison, we can reach the following conclusions: (1) The *in situ* stress has the greatest effect on reflection coefficient and transmission coefficient at the interface of two sandstones, followed by the interface between sandstone and limestone, and has the least effect on the interface between sandstone and granite or tight rock. (2) When the dry rock is filled with fluid, the effect of *in situ* stress on the reflectivity and transmissivity at all interfaces is slightly reduced. The reflection and transmission of *SV* wave are almost not affected by the *in situ* stress. (3) The model test shows that the *in situ* stress has the most significant effect on the *P*-wave reflection coefficient, but has almost no effect on the *SV*-wave transmission coefficient.

When the normal *in situ* stress becomes zero, eq. (28) can be degenerated to the classic Zoeppritz equation, which preliminarily proves the correctness of the proposed eq. (28). Previous studies on the reflection and transmission coefficients of energy have shown that the critical incident angle decreases with the increase of normal *in situ* stress when the upper and lower layers are sandstone, which is consistent with observed phenomenon in this paper. This can further verify the proposed equations.

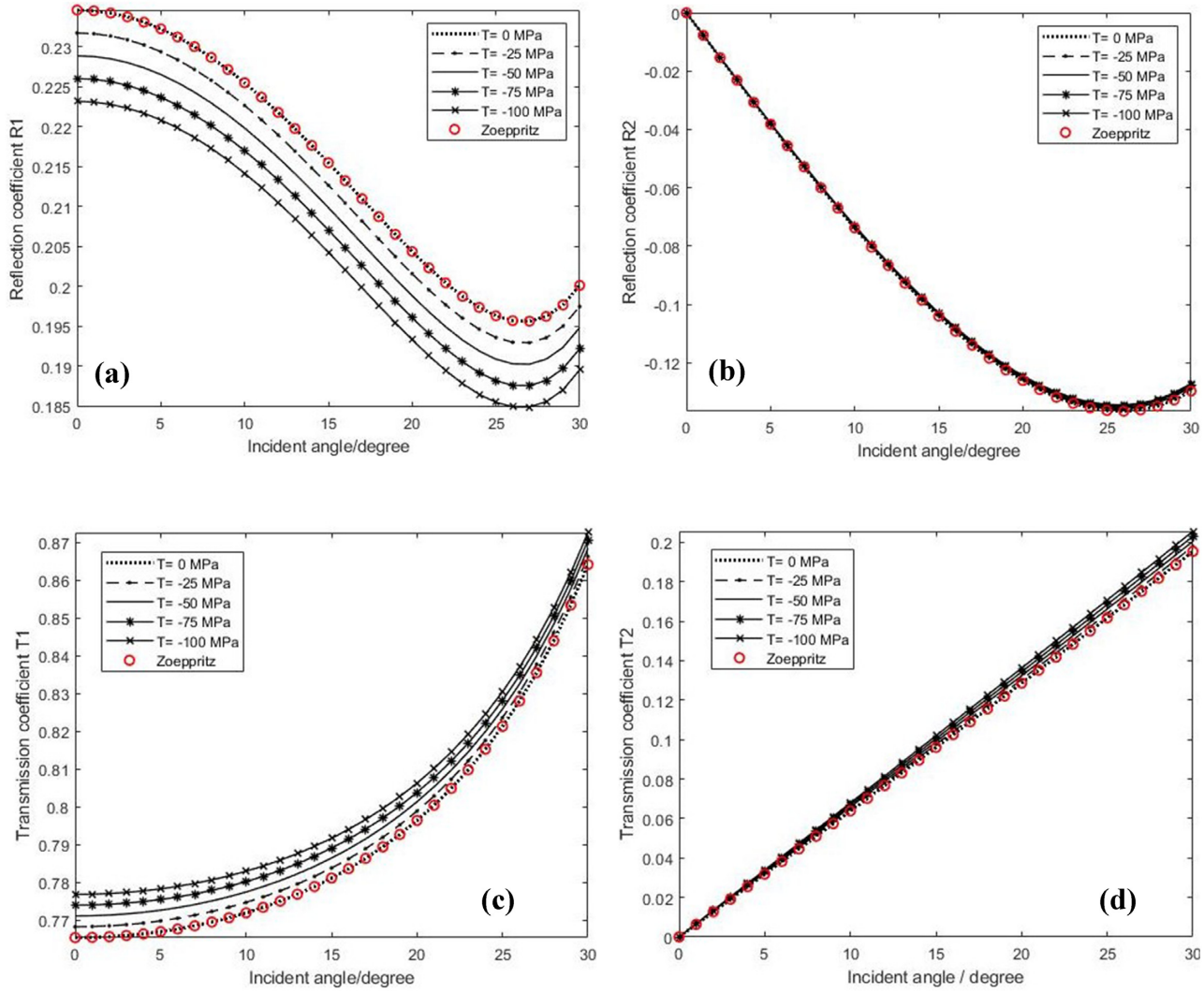

Figure 15. The seismic reflection coefficients and transmission coefficients at the interface between saturated Castlegate sandstone and saturated Berea3 sandstone under normal *in situ* stress. The dotted, dashed, solid, star marked and cross marked lines denote unstressed state, −25, −50, −75 and −100 MPa in rocks, respectively; the red hollow circle denotes the Zoeppritz equation. (a) Reflection coefficient of *P* wave, (b) reflection coefficient of *SV* wave, (c) transmission coefficient of *P* wave and (d) transmission coefficient of *SV* wave.

ACKNOWLEDGEMENTS

We would like to acknowledge the sponsorship of National Natural Science Foundation of China (41974119 and 42030103). We also thank the anonymous reviewers for their constructive suggestions.

DATA AVAILABILITY

The data underlying this paper are available in the paper and in its online supplementary material.

REFERENCES

Abdideh, M. & Moghimzadeh, M., 2019. Geomechanical study of gas reservoir rock using vertical seismic profile and petrophysical data (continental shelf in southern Iran), *Geomech. Geoeng.,* **14,** 118–135.

Abiza, Z., Destrade, M. & Ogden, R.W., 2012. Large acoustoelastic effect, *Wave Motion,* **49,** 364–374.

Aki, K. & Richards, P., 1980. *Quantitative Seismology,* W. H. Freeman.

Chen, H., Li, J. & Innanen, K., 2020. Nonlinear inversion of seismic amplitude variation with offset for an effective stress parameter, *Geophysics,* **85,** 1–74.

Degtyar, A.D., 1998. Stress effect on boundary conditions and elastic wave propagation through an interface between anisotropic media, *J. acoust. Soc. Am.,* **104,** 1992–2003.

Degtyar, A.D. & Rokhlin, S.I., 1995. Absolute stress determination in orthotropic materials from angular dependences of ultrasonic velocities, *J. Appl. Phys.,* **78,** 1547–1556.

Fatti, J.L, 1994. Detection of gas in sandstone reservoirs using AVO analysis: a 3-D seismic case history using the Geostack technique, *Geophysics,* **59,** 1362–1376.

Hughes, D.S. & Kelly, J.L., 1953. Second-order elastic deformation of solids, *Phys. Rev.,* **92,** 1145–1149.

Liu, J., Cui, Z. & Wang, K., 2010. The relationships between uniaxial stress and reflection coefficients, *Geophys. J. Int.,* **179,** 1584–1592.

Liu, J., Cui, Z. & Wang, K., 2012. Effect of stress on reflection and refraction of plane wave at the interface between fluid and stressed rock, *Soil Dyn. Earthq. Eng.,* **42,** 47–55.

Norris, A.N., 1995. The speed of a wave along a fluid/solid interface in the presence of anisotropy and prestress, *J. acoust. Soc. Am.,* **98,** 1147–1154.

Pao, Y.H., Sache, W. & Fukuoka, H., 1984. Acoustoelasticity and ultrasonic measurement of residual stress, *Phys. Acoust.,* **15,** 61–143.

Prioul, R., Smith, G.C., Vail, P.J., Strauss, P.J. & Levitt, P.R., 2004. Analytic insight into shear-wave AVO for fractured reservoirs, in *74th Annual International Meeting, Society of Exploration Geophysicists, Expanded Abstracts,* pp. 1801–1804.

Rasolofosaon, P., 1998. Stress–induced seismic anisotropic revisited, *Rev. Inst. Fr. Petrole,* **53,** 679–692.

Robert, E. & Lloyd, P., 1983. *Exploration Seismology,* Cambridge Univ. Press.

Simmons, G., 1964. Velocity of shear waves in rocks to 10 kilobars, *J. geophys. Res,* **69,** 1123–1130.

Shuey, R.T., 1985. A simplification of the Zoeppritz equations, *Geophysics,* **50,** 609–614.

Song, G., Du, X., Lv, Y., Shi , Y., Zhang, B. & He, F., 2020. A new method for characterizing the acoustoelastic effect of the acoustic reflection/transmission coefficient of the liquid-solid interface of pre-stressed thin plate materials. *Chin. J. Mech. Eng.,* **56,** 1–7.

Tatsuo, T. & Masakatsu, S., 1969. Elastic wave propagations and acoustical birefringence in stressed crystals, *J. acoust. Soc. Am.,* **45,** 1241–1246.

Tian, J. & Hu, L., 2010. Progress in theories and experimental technologies of solid acoustoelasticity and its application, *Adv. Mech.,* **40,** 652–662.

Tian, J. & Wang, E., 2006. Ultrosonic method for measuring in-situ stress based on acoustoelasticity theory, *Chin. J. Rock Mech. Eng.,* **25,** 1–6.

Wang, Y., 2012. Approximations to the Zoeppritz equations and their use in AVO analysis, *Geophysics,* **64,** 1920–1927.

Wang, Z., 2002. Seismic anisotropy in sedimentary rocks, part 2: laboratory data, *Geophysics,* **67,** 1423–1440.

Wang, Z. & Wang, R., 2015. Pore pressure prediction using geophysical methods in carbonate reservoirs: current status, challenges and way ahead, *J. Nat. Gas Sci. Eng.,* **27,** 986–993.

Winkler, K.W. & Larry, M., 2004. Nonlinear acoustoelastic constants of dry and saturated rocks, *J. geophys. Res,* **109,** 1–9.

Yin, X., Zong, Z. & Wu, G., 2015. Research on seismic fluid identification driven by rock physics, *Sci. China Earth Sci.,* **58,** 159–171.

Zhang, J., 2013. Effective stress, porosity, velocity and abnormal pore pressure prediction accounting for compaction disequilibrium and unloading, *Mar. Pet. Geol.,* **45,** 2–11.

Zong, Z., Yin, X. & Wu, G., 2013. Direct inversion for a fluid factor and its application in heterogeneous reservoirs, *Geophys. Prospect.,* **61,** 998–1005.